International Immunology, Vol. 33, No. 3, pp. 171–182
doi:10.1093/intimm/dxaa069
Advance Access publication 10 October 2020

Selective expression of claudin-5 in thymic endothelial cells regulates the blood–thymus barrier and T-cell export

Takahiro Nagatake[1,2], Yan-Chun Zhao[3], Takeshi Ito[1,4], Masahiko Itoh[5], Kohei Kometani[4], Mikio Furuse[6,7], Azusa Saika[2,8], Eri Node[2], Jun Kunisawa[2,8], Nagahiro Minato[1,3,9] and **Yoko Hamazaki[1,4]**

[1]Department of Immunology and Cell Biology, Graduate School of Medicine, Kyoto University, Kyoto 606-8501, Japan
[2]Laboratory of Vaccine Materials, Center for Vaccine and Adjuvant Research and Laboratory of Gut Environmental System, National Institutes of Biomedical Innovation, Health and Nutrition (NIBIOHN), Osaka 567-0085, Japan
[3]Graduate School of Biostudies, Kyoto University, Kyoto 606-8501, Japan
[4]Laboratory of Immunobiology, Graduate School of Medicine, Center for iPS Cell Research and Application (CiRA), Kyoto University, Kyoto 606-8507, Japan
[5]Department of Biochemistry, School of Medicine, Dokkyo Medical University, Tochigi 321-0293, Japan
[6]Division of Cell Structure, National Institute for Physiological Sciences, Okazaki, Aichi 444-8787, Japan
[7]Department of Physiological Sciences, SOKENDAI, The Graduate University for Advanced Studies, Okazaki, Aichi 444-8787, Japan
[8]Graduate School of Pharmaceutical Sciences, Osaka University, Osaka 565-0871, Japan
[9]Medical Innovation Center, Kyoto University, Kyoto 606-8507, Japan

Correspondence to: Y. Hamazaki; E-mail: yoko.hamazaki@cira.kyoto-u.ac.jp

Received 3 October 2019, *editorial decision* 1 October 2020; *accepted* 8 October 2020

Abstract

T-cell development depends on the thymic microenvironment, in which endothelial cells (ECs) play a vital role. Interestingly, vascular permeability of the thymic cortex is lower than in other organs, suggesting the existence of a blood–thymus barrier (BTB). On the other hand, blood-borne molecules and dendritic cells bearing self-antigens are accessible to the medulla, facilitating central tolerance induction, and continuous T-precursor immigration and mature thymocyte egress occur through the vessels at the cortico-medullary junction (CMJ). We found that claudin-5 (Cld5), a membrane protein of tight junctions, was expressed in essentially all ECs of the cortical vasculatures, whereas approximately half of the ECs of the medulla and CMJ lacked Cld5 expression. An intravenously (i.v.) injected biotin tracer hardly penetrated cortical Cld5^{+} vessels, but it leaked into the medullary parenchyma through Cld5^{-} vessels. Cld5 expression in an EC cell line caused a remarkable increase in trans-endothelial resistance *in vitro*, and the biotin tracer leaked from the cortical vasculatures in *Cldn5*$^{-/-}$ mice. Furthermore, i.v.-injected sphingosine-1 phosphate distributed selectively into the medulla through the Cld5^{-} vessels, probably ensuring the egress of CD3^{high} mature thymocytes from Cld5^{-} vessels at the CMJ. These results suggest that distinct Cld5 expression profiles in the cortex and medulla may control the BTB and the T-cell gateway to blood circulation, respectively.

Keywords: endothelial barrier, sphingosine-1 phosphate, thymus, tight junction

Introduction

The thymus provides a crucial microenvironment for T-lymphocyte development and consists of two distinct anatomical and functional compartments, the cortex and medulla. Thymic epithelial cells (TECs) function as a major stromal component by expressing self-peptide–major histocompatibility complex (MHC) complexes as well as various cytokines and chemokines to support thymocyte development, selection and migration (1, 2). T-progenitors enter the thymus, proliferate and express the co-receptors CD4 and CD8 as well as their own unique T-cell receptors (TCRs). Thymocyte clones bearing low-affinity TCRs to self-peptide–MHC complexes are positively selected by cortical TECs (cTECs) and become CD4 or CD8 single positive (SP) thymocytes. SP cells then migrate into the medulla (3, 4), where medullary

TECs (mTECs) expressing self-antigens and dendritic cells (DCs) cooperatively delete autoreactive T cells (negative selection) (5).

Blood vessels are another important stromal component that ensures the supply of oxygen and nutrients as well as the import and export of various cellular and serum components (6–8). The thymic vascular network is morphologically characterized by cortical capillaries, medullary arterioles and postcapillary venules (PCVs) in the medulla and corticomedullary junction (CMJ) (7, 9–12). The immigration of T-cell precursors and emigration of mature SP thymocytes are mediated by specified blood vessels at the CMJ (3, 8–11, 13–19). Importantly, the egress of SP thymocytes depends on a lipid mediator, sphingosine-1 phosphate (S1P) (20), and a defect in the S1P-S1P1 (a S1P receptor) axis results in immunodeficiency due to a significant reduction of T-cell export from the thymus (21–23). The concentration of S1P is maintained at a higher level in blood and lymph and lower level in tissue parenchyma, thereby generating a S1P gradient for leukocyte trafficking (24). Although it is known that blood-borne S1P is important for the egress of mature SP thymocytes (17), how plasma-derived S1P penetrates blood vessels and distributes in the thymic tissue parenchyma has not been clarified.

The unique properties of thymic blood vessels have been suggested to contribute to the functional integrity of the cortex and medulla. In 1961, Marshall's group found that thymic vascular permeability was relatively low compared with other tissues, leading them to propose the concept of the blood–thymus barrier (BTB), which assures the selection process by excluding circulating antigens (25). In 1972, Raviola and Karnovsky showed that intravenously (i.v.)-injected tracer molecules were distributed into the medullary region, suggesting that the barrier exists only in the cortex compartment (9). Thereafter, accumulating evidence has indicated that blood-borne molecules and cells are accessible specifically to the medulla. For example, blood-borne antigens directly enter the thymus and are captured by thymic DCs abundantly localized in the medulla, and peripheral DCs transport peripheral antigens by their migration into the thymic medulla; both these phenomena play important roles in establishing central T-cell self-tolerance by the induction of negative selection and generation of Foxp3$^+$ T-regulatory (T_{reg}) cells (26–30). Furthermore, it was found that the conduit, which is a unique extracellular matrix (ECM)-based network, can transport blood-borne small molecules or chemokines to defined locations within the medulla (31). These observations have modified the initial concept of the BTB; the thymic medulla actively opens to blood circulation, which may enhance DC-mediated self-tolerance against circulating self-antigens. However, the molecular basis that ensures the different vascular permeabilities between the cortex and medulla remains to be elucidated.

Blood vessels are composed of endothelial cells (ECs), pericytes, smooth muscle cells, basement membranes and cell–cell junctions between the ECs, all of which are crucial determinants of vascular permeability. Endothelial tight junctions (TJs) are constituted of membrane proteins, including claudins (Clds), occludin, junctional adhesion molecule (JAM) and endothelial cell-selective adhesion molecules (ESAM), and of intracellular molecules, including ZO-1 (32, 33). Among these constituents, Clds at the TJs play a major role in regulating paracellular permeability. Clds are tetra-spanning membrane proteins which constitute more than 20 subfamilies and are differently expressed depending on the cell type in various tissues (34). Among them, Cld5 is preferentially expressed in brain ECs (35), whereas there has been argument about Cld12 being preferentially expressed in brain ECs (36). It is well known that blood vessels in the brain show low permeability, a phenomenon termed the blood–brain barrier (BBB) (37, 38). Importantly, Cld5 is strongly and selectively expressed in almost all ECs of the brain, and its absence (*Cldn5*$^{-/-}$ mice) results in a leaky BBB, leading to lethality soon after birth (39). Thus, although vascular permeability is regulated by various factors (32, 33), Cld5 expression in brain ECs is essential for the establishment of the BBB (39).

In this study, we examined the Cld expression in thymic ECs to clarify a mechanism ensuring low permeability and high leakiness in cortical and medullary blood vessels, respectively. We found that Cld5 is selectively expressed in thymic ECs of the cortical compartment and plays a crucial role in establishing the BTB. In addition, blood-borne molecules including plasma-derived S1P and mature SP thymocytes are imported and exported respectively from Cld5$^-$ blood vessels at the medulla/CMJ, suggesting that the specific absence of Cld5 may assure a specific gateway to the blood circulation.

Methods

Mice

C57BL/6 wild-type (WT) mice were purchased from Japan SLC (Shizuoka, Japan). *Cld5*$^{-/-}$ mice were generated as described previously (39). Animals were maintained in specific pathogen-free conditions at the Kyoto University Laboratory Animal Centers or the National Institutes of Biomedical Innovation, Health and Nutrition. Mice between 6 and 8 weeks of age were used unless otherwise mentioned. This study was performed in accordance with the principles expressed in the Declaration of Helsinki and approved by the Animal Research Committee, Graduate School of Medicine, Kyoto University (MedKyo16596 and 17-96-14) and the Animal Care and Use Committee and Ethics of Animal Experiments Committee of the National Institutes of Biomedical Innovation, Health and Nutrition (DSR01-2).

Antibodies

The antibodies and reagents used for the immunohistological analysis were as follows: Alexa Fluor 488-conjugated-anti-Cld5 mAb (4C3C2; Invitrogen/Thermo Fisher Scientific, Waltham, MA, USA), anti-Cld5 pAb (34-1600; Invitrogen/Thermo Fisher Scientific), anti-Cld12 pAb (35), Cy3-conjugated anti-α-SMA mAb (1A4; Sigma-Aldrich/Merck KGaA, Darmstadt, Germany), anti-CD31 mAb (MEC13.3; BD, San Jose, CA, USA), anti-CD3ε mAb (145-2C11; BioLegend, San Diego, CA, USA), biotinylated-UEA-1 (Vector Laboratories, Burlingame, CA, USA), Fluorescein-UEA-I (Vector Laboratories), anti-laminin pAb (Millipore/Merck KGaA), anti-collagen IV pAb (Millipore/Merck KGaA), anti-ZO1 pAb (Invitrogen/Thermo Fisher Scientific), anti-ESAM mAb (1G8; BioLegend), Alexa Fluor 488-conjugated anti-JAM-A mAb (H202-106; AbD Serotec/Bio-Rad, Hercules, CA, USA), anti-occludin pAb (Zymed/Thermo Fisher Scientific), anti-VE-cadherin pAb (Santa Cruz Biotechnology, Dallas,

TX, USA), Cy3-, Alexa Fluor 546- and Alexa Fluor 647-conjugated anti-rat, -rabbit and -goat IgG (Invitrogen/Thermo Fisher Scientific) and streptavidin (Invitrogen/Thermo Fisher Scientific). The following antibodies were used for western blotting: anti-Cld5 pAb (IBL, Gunma, Japan) and anti-actin pAb (Santa Cruz Biotechnology). The following antibodies were used for FACS analysis. APC-conjugated CD8α mAb (53-6.7; BioLegend), phycoerythrin (PE)-Cy7-conjugated CD4 mAb (GK1.5; BioLegend), BV421-conjugated CD45 mAb (30-F11; BioLegend), BV421-conjugated Ter119 (TER119; BioLegend), APC-conjugated CD31 (390; BioLegend), PE-Cy7-conjugated EpCAM (G8.8; BioLegend) and Alexa Fluor 488-conjugated-anti-Cld5 mAb (4C3C2; Invitrogen/Thermo Fisher Scientific).

Immunohistochemistry

Histological analysis was performed as previously described (40) with some modification. Tissues samples were frozen with liquid nitrogen in Tissue-Tek OCT compound (Sakura, Tokyo, Japan) or fixed with 10 N formalin (Wako, Osaka, Japan) overnight at 4°C. Fixed samples were then dehydrated with 10% and 20% (w/v) sucrose solution before being frozen. Freshly prepared cryostat sections (6 μm) were fixed with 95% ethanol for 30 min at 4°C, followed by 100% acetone for 1 min at room temperature. After being blocked with 2% (v/v) fetal calf serum (FCS) in phosphate-buffered saline (PBS) for 30 min at room temperature, pre- or post-fixed samples were incubated with primary antibodies or reagents for 16 h at 4°C. Each sample was then washed with 0.1% Tween PBS and PBS for 5 min, followed by staining with secondary reagents for 30 min at room temperature. Finally, all samples were washed with PBS two times, mounted in Mowiol (Calbiochem/Merck KGaA) and examined under a fluorescence photo microscope (Axiovert 200M; Carl Zeiss, Oberkochen, Germany). In some experiments, the samples were counterstained with DAPI (Sigma-Aldrich/Merck KGaA) to visualize the nucleus. For quantification of the histological analysis, Cld5$^+$ and Cld5$^-$ and/or CD3ε$^+$ and CD4$^+$ T cell-attaching blood vessels in one thymic lobe were counted. The cortex and medullary borders were defined by DAPI staining, and the CMJ area was defined as 100 μm from the cortical side of the border. Data from at least three sections were accumulated, and the percentage of blood vessels with their indicated characteristics among all thymic blood vessels in each region was calculated.

Analysis of thymocyte development by flow cytometry

Thymocytes were washed through a 70-μm cell strainer and counted. After blocking antibody treatment for 5 min at room temperature (anti-CD16/32 mAb; 2.4G2; BD), the samples were stained with CD4 and CD8α antibodies for 30 min at 4°C. The percentage of dead cells was evaluated by PI staining. Samples were examined by FACSCanto (BD) or SA3800 (SONY, Tokyo, Japan), and data analysis was performed with FlowJo software (Treestar Inc., San Carlos, CA, USA).

Flow cytometric analysis of thymic stromal cell fraction

The isolation of thymic stromal cells was performed as previously described (41, 42). Briefly, thymic lobes were minced into small pieces and gently agitated to release thymocytes. After settling the fragments, the thymocyte-rich fraction was discarded, and the remaining fragments were digested using 0.5 U ml^{-1} Liberase™ (Roche, Basel, Switzerland) and 0.2 mg ml^{-1} DNase I (Roche) in RPMI media at 37°C for 10 min with gentle agitation every 5 min until a single-cell suspension was formed. After settling the fragments, the supernatants were transferred to a new tube, and the remaining fragments, which were enriched with TECs, were further digested with enzymes at 37°C for 10 min as described above. The supernatant and TEC-rich fraction were pooled and passed through a 70-mm filter. The cell suspension was centrifuged and resuspended in PBS supplemented with 5 mM EDTA and 1% FCS (hereafter FACS buffer), and blocked with anti-FcYRIIb for 20 min at 4°C. The samples were stained with CD45, Ter119, CD31 and EpCAM antibodies for 30 min on ice. For intracellular staining of claudin-5, after washing twice with 2% FCS PBS, the cells were fixed and permeabilized using cytofix/cytoperm solution (BD) for 20 min on ice, washed with 1× perm/wash buffer (BD) twice and stained with anti-Cld5 antibody for 30 min on ice. The samples were then examined and analyzed as described above. The EC and TEC fractions were defined as CD31$^+$ and EpCAM$^+$ populations, respectively, in the CD45$^-$ Ter119$^-$ stromal cell fraction.

Tracer experiments

Tracer experiments were performed as previously described (39) with some modifications. Six- to 8-week-old C57BL/6 WT mice were intravenously injected with 200 μl of the following tracer reagents with a 27G needle (Terumo, Tokyo, Japan): 2 mg ml^{-1} EZ-Link™ Sulfo-NHS-SS-Biotin (MW: 607, Pierce Chemical, Dallas, TX, USA) in PBS containing 1 mM $CaCl_2$ or 175 mg ml^{-1} tetramethylrhodamine-conjugated S1P (MW: 807, Echelon Biosciences, Salt Lake City, UT, USA) in methanol/PBS containing 1 mM $CaCl_2$. In the analysis of *Cld5*$^{-/-}$ mice, *Cld5*$^{+/-}$ intercross littermates were obtained at E18.5 and were injected with 20 μl of 2 mg ml^{-1} EZ-Link™ Sulfo-NHS-SS-Biotin in PBS containing 1 mM $CaCl_2$ via the facial vein route with a 33G needle (Hamilton, Reno, NV, USA). Thymi were examined by immunohistochemistry 20 min after the injection of a biotin tracer and 5–30 min after the injection of tetramethylrhodamine-conjugated S1P, respectively.

Intravascular labeling of egressing thymocytes

An intravascular thymocyte labeling assay was conducted as previously described (43). CD4 SP thymocytes were labeled *in vivo* by the injection of 6-week-old C57BL/6 WT mice with 1 μg of PE-conjugated rat anti-mouse CD4 antibody (RM4-5; BD) intravenously. Three to 30 min later, mice were euthanized and intravascularly perfused with PBS and subsequently with 4% paraformaldehyde (Wako). Thymi were post-fixed with 4% paraformaldehyde for 2 h at 4°C and dehydrated as described above.

FTY720 treatment

To inhibit thymocyte egress, mice were treated with FTY720 (Cayman Chemical, Ann Arbor, MI, USA) as previously described (44) with some modifications. In brief, 6-week-old C57BL/6 WT mice were treated with FTY720 (1 mg kg^{-1} i.p.) or 0.5% (v/v) ethanol in PBS for 25 consecutive days. Thymi were collected 24 h after the final FTY720 treatment and examined by immunohistochemistry.

Cell culture

The SVEC 4-10 endothelial cell line was established previously (45). The cells were cultured in DMEM (high glucose) with 10% FCS, 2 mM L-glutamine, 1 mM sodium pyruvate, 100 U ml^{-1} penicillin, 100 mg ml^{-1} streptomycin, 0.1 mM Non-Essential amino acid, 60 mM 2-ME and 20 mM HEPES. All culture surfaces were coated with 0.1% gelatin. The cells were counted and seeded at 3×10^5 per dish (10 cm) at every passage and maintained in 95% air and 5% CO_2 at 37°C.

Transfection of claudin-5 in SVECs

The entire mouse Cld5 open reading frame cDNA was obtained by RT-PCR and ligated with pMCs-IRES-EGFP retroviral vector after purification. pMCs-IRES-EGFP-Cld5 (F147A), in which phenylalanine at position 147 of mouse claudin-5 was substituted with alanine, was generated by inverse PCR using the primers 5'-CGCGAGGCCTATGATCCGACGGTGCCGGTGTCA-3' and 5'-ATCATAGGCCTCGCGGACAACGATGTTGGCGAA-3'. PLAT-E cells were transfected either with EGFP control retroviral vectors or Cld5- or Cld5 (F147A)-ligated retroviral vectors using Lipofectamine 2000 (Invitrogen/Thermo Fisher Scientific), and the medium was changed the next day. On the following day, the retroviral particle-containing supernatants were harvested and filtered through a 0.45-μm filter (Millipore/Merck KGaA). SVECs were infected by the virus supernatants. After culturing for 1 week, the infected cells were selected based on the EGFP expression by using FACSAria (BD).

RT-PCR

Total RNAs from confluently cultured cells were isolated with Trizol (Invitrogen/Thermo Fisher Scientific). Then they were used to generate cDNAs by reverse transcription. The primer sequences of Cld5 and CD31 for the PCR were as follows: Cld5, (forward) 5' -CAGGATCCACCATGGGGTCTGCAGCGTTGG-3', (reverse) 5' -ACGAATTCTTAGACATAGTTCTTCTTGT-3'; CD31, (forward) 5' -CCCACCGAAAGCAGTAATC-3', (reverse) 5' -CCCAGAAAGAAGAGAACAACAG-3'; and HPRT, (forward) 5' -GGGGGCTATAAGTTCTTTGC-3', (reverse) 5' -TCCAACACTTCGAGAGGTC-3'.

Western blotting

To make protein samples, SVECs, EGFP-SVECs and $Cld5^+$-SVECs were cultured until confluent. The cells were washed once with PBS then lysed directly with 400 μl RIPA buffer [150 mM NaCl, 25 mM Tris–HCl (pH 7.6), 1% NP-40, 1% sodium deoxycholate, 0.1% SDS, protease and phosphatase inhibitors] for 30 min on ice. The lysates were centrifuged, and the supernatants containing proteins were collected. Twenty milligrams of total proteins were loaded for sodium dodecyl sulfate–polyacrylamide gel electrophoresis (SDS–PAGE) with stacking gel and 10% separation gel. Proteins were transferred to PVDF membrane and blocked with 5% skimmed milk for 1 h.

Transepithelial electrical resistance measurement

SVECs stably expressing the control vector, Cldn5-ligated vector or Cldn5 F147A-ligated vector were seeded on transwells (Corning, NY, USA, 3413, pore size 0.4 μm, growth surface area 0.33 cm^2) at 5×10^4 cells per well. Electric resistance (R) was measured with Millicell ERS-2 (Millipore/Merck KGaA) 5 days after cell seeding. The medium was changed every 2 days. Transepithelial electrical resistance (TER) was calculated by the following equation: $(R_{cells} - R_{membrane\ only}) \times$ growth surface area ($\Omega \bullet cm^2$).

Electron microscopy

Mice were intravascularly perfused with 2% glutaraldehyde, 4% paraformaldehyde and 0.1 M sodium phosphate buffer (pH 7.4), followed by additional fixation with the same solution for 16 h at 4°C. The samples were then fixed with 1% osmium tetraoxide for 2 h, followed by dehydration with a series of ethanol gradients. The tissues were embedded in Epon 812 Resin mixture, and ultrathin (80 nm) sections were cut on an Ultra microtome EM UC6 (Leica, Vienna, Austria). The ultrathin sections were stained with 2% uranyl acetate in 70% ethanol for 5 min at room temperature and then in Reynold's lead citrate for 5 min at room temperature. Sections were analyzed with a Hitachi H-7650 transmission electron microscope (Hitachi, Tokyo, Japan).

Statistical analysis

Results were compared with the Student's *t*-test by using GraphPad Prism (GraphPad Software, San Diego, CA, USA). Data are presented as the mean and standard errors of the mean (SEM) unless indicated otherwise.

Results

Unique expression of claudin-5 in thymic blood vessels

Since Cld5 is expressed in all ECs in the brain and plays a crucial role in establishing the BBB (39), we first examined the expression and distribution of Cld5 in the adult thymus by co-staining with an EC marker, CD31 (46). Most $CD31^+$ blood vessels in the thymus expressed Cld5, but a portion of them in the medulla and CMJ were $Cld5^-$ (Fig. 1A). Notably, all small-diameter blood vessels in the cortex, which are presumably capillaries (11, 12), strongly expressed Cld5 (Fig. 1A), whereas Cld12 was not detected in thymic ECs (Supplementary Figures S1 and S3). Quantification analysis indicated that approximately 60% (61.7 ± 5.3 %) and more than 90% (93.6 ± 1.1 %) of blood vessels in the medulla/CMJ and cortex were $Cld5^+$, respectively (Fig. 1B). In a more detailed analysis, α-SMA^+ arterioles at the CMJ expressed Cld5, whereas α-SMA^- large-diameter vessels located near the arterioles, which were presumably PCVs (11), lacked the Cld5 expression (Fig. 1C). Occludin, which is another membrane protein of TJs and expressed in all ECs in the brain (39), was expressed only in $Cld5^+$ arterioles at the CMJ (Supplementary Figures S2 and S3). Other molecules constituting endothelial junctions including ZO-1, ESAM-1, JAM-A and VE-cadherin (33, 47) were expressed in all blood vessels in the thymus (Supplementary Figures S2 and S3). These results indicated that thymic blood vessels showed heterogeneity based on their localization and expression of junctional molecules (Supplementary Figure S3). In addition, Cld5 showed a unique expression pattern: Cld5 was expressed in all capillaries in the thymic cortex and arterioles, whereas blood vessels including PCVs in the medulla/CMJ lacked Cld5 expression (Supplementary Figure S2).

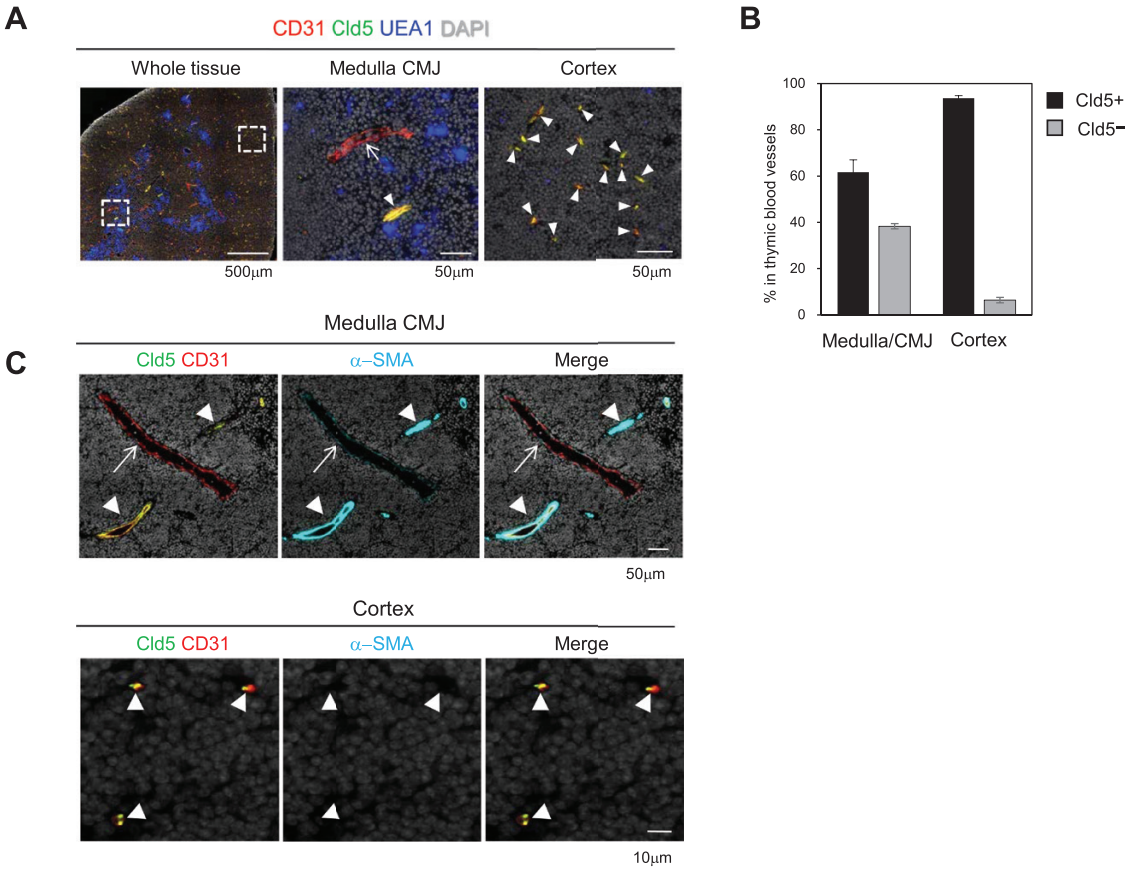

Fig. 1. Heterogeneous expression of claudin-5 in thymic blood vessels. (A) The thymi of 6- to 8-week-old wild type (WT) C57BL/6 (B6) mice were three-color stained with anti-CD31 antibody, anti-Cld5 antibody and UEA1 (a medulla marker). (B) The percentages of Cld5$^+$ and Cld5$^-$ blood vessels in the medulla/CMJ or cortex are indicated. Data are presented as the mean and SEM. (C) The WT thymi were three-color stained with anti-CD31 antibody, anti-Cld5 antibody and anti-α-SMA antibody. Arrowheads and arrows indicate Cld5$^+$ and Cld5$^-$ vessels, respectively. These data are representative of at least three independent experiments.

Cld5 expression in thymic ECs

We then examined Cld5 expression in thymic cell populations by flow cytometry (FCM). The thymus was enzymatically digested into single cells, and intracellular staining using mouse anti-claudin-5 mAb was performed as described in the "Methods" section. Almost no signal was detected in CD45$^+$ hematopoietic cell populations (data not shown). Cld5 signals were clearly detected in the EC fraction (CD31$^+$EpCAM$^-$) within the stromal fractions (CD45$^-$Ter119$^-$) of *Cldn5*$^{+/+}$ mice, slightly less so in *Cldn5*$^{+/-}$ ECs, and completely abolished in *Cldn5*$^{-/-}$ ECs (Fig. 2A), confirming the specificity of Cld5 staining by FCM. TEC fractions also showed quite a low level of Cld5 staining (Fig. 2A). However, these signals could still be detected in *Cldn5*$^{-/-}$ mice (Fig. 2A), indicating the Cld5 signals in TECs detected by FCM might be due to non-specific binding or cross-reactions with other claudin family members expressed in mTECs such as Cld3 and Cld4 (40, 42). Using this method, we analyzed the Cld5 expression in ECs at various ages. Almost all ECs were Cld5$^+$ on embryonic day (E)14.5 (Fig. 2B and Supplementary Figure S4). Cld5$^-$ blood vessels were first detected, by immunohistochemistry, around E17.7-E18.5, when the medulla becomes expanded, although the percentage of Cld5$^-$ ECs in the FCM analysis was still only around 1.5% (Fig. 2B and Supplementary Figure S4). Cld5$^-$ fractions were obviously detected in ECs from 3-week-old thymus by FCM, and approximately 80% of CD31$^+$ ECs expressed Cld5 in adult (9 weeks old) thymus. The Cld5$^+$ proportion as well as the Cld5 intensity gradually decreased thereafter and significantly decreased in aged mice (2 years old) (Fig. 2B). These results indicate that Cld5 is specifically expressed in ECs in the thymus and that Cld5$^-$ blood vessels develop and are accompanied by medulla expansion.

Cld5 directly controls the paracellular permeability of ECs via its TJ-forming capability

To examine whether the expression of Cld5 could directly control paracellular permeability between ECs, we examined the effect of Cld5 expression in ECs on the trans-epithelial resistance (TER). A SVEC line that shows no detectable Cld5 proteins (Fig. 3A and B) was retrovirally transfected with either *EGFP* (Cont) or *Cldn5* (Cld5) using the pMCs-IRES-GFP vector. In addition, to clarify whether the TJ-forming capability of Cld5 is required for the regulation of paracellular permeability, a *Cldn5* mutant (Cld5 F147A), which can localize at the plasma membranes but lacks the ability to form TJ strands (48), was generated and retrovirally introduced into the SVEC

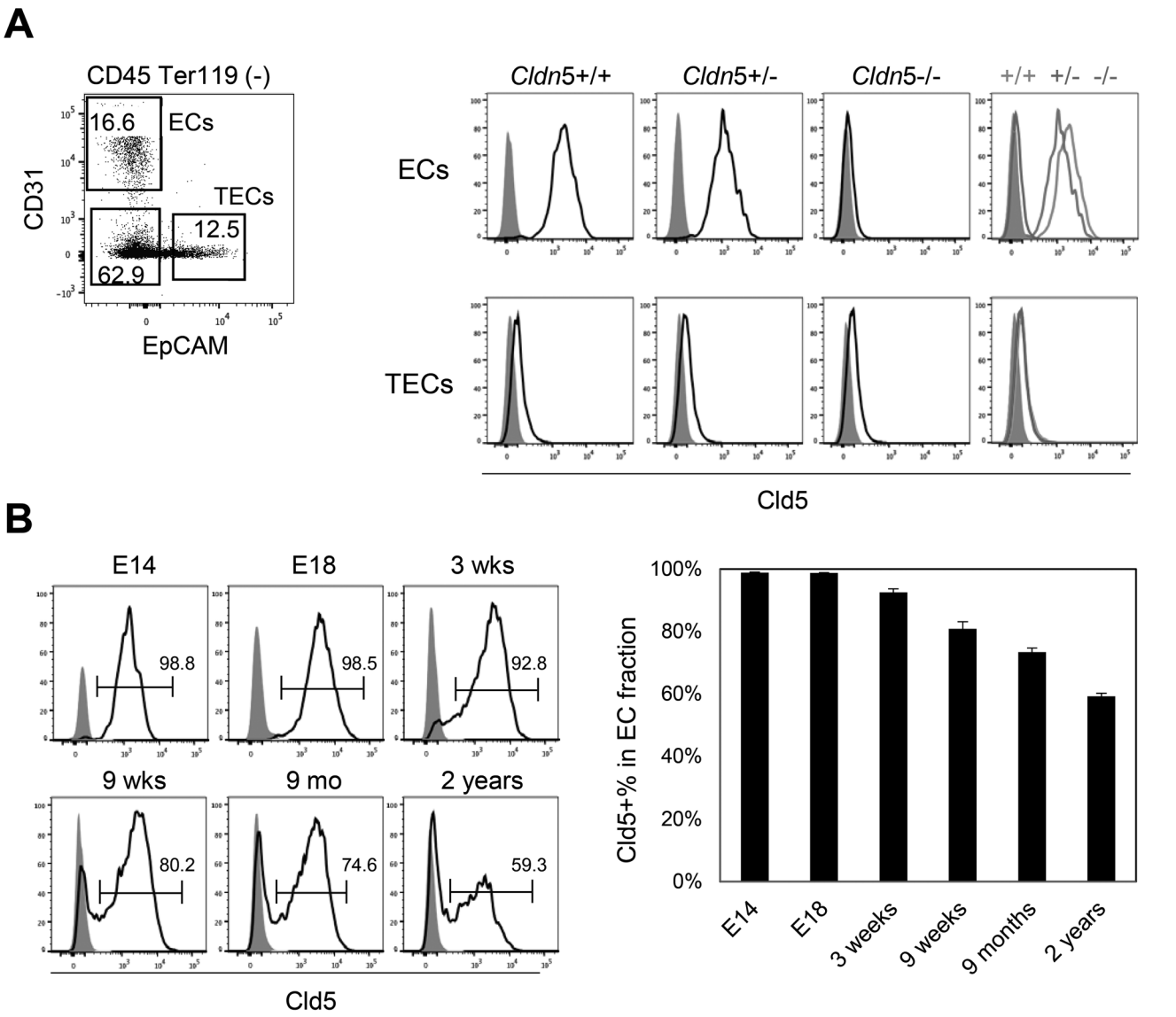

Fig. 2. Claudin-5 expression in thymic endothelial cells. (A) Gating strategy of thymic CD31⁺ endothelial cells (ECs) and EpCAM⁺ epithelial cells (TECs) in the CD45⁻Ter119⁻ stromal cell fraction using flow cytometry (FCM) (left). The expression of Cld5 in ECs and TECs of *Cldn5*$^{+/+}$, *Cldn5*$^{+/-}$ and *Cldn5*$^{-/-}$ E18 thymi were analyzed by FCM (right). (B) The expression of Cld5 in thymic ECs at the indicated ages was analyzed by FCM (left). Data are presented as means and SEM using at least three mice (right). FCM plots are representative of at least three independent experiments in (A) and (B).

line. Cld5 proteins were detected in *Cldn5*- and *Cldn5* F147A-transfected SVECs, but not in control vector-transfected SVECs, confirming that Cld5⁺ and Cld5⁻ SVEC lines were established (Fig. 3A and B). Immunofluorescence microscopy analysis showed that Cld5 and Cld5 F147A were similarly localized at cell–cell contact sites (Fig. 3A), as shown previously (35, 48). Importantly, Cld5-expressing SVECs showed significantly higher TER than control or Cld5 F147A-expressing SVECs (Fig. 3C). These data indicate that Cld5 directly controls the paracellular permeability of ECs via its TJ-forming capability and suggest a role for the BTB in the cortex.

Disruption of BTB in Cld5$^{-/-}$ *mice*

We next directly examined the role of Cld5 on BTB function *in vivo* and thymocyte development using *Cld5*$^{-/-}$ mice. Because of the early lethality (within 10 h after birth) (39), thymic phenotypes on E18 were examined. Immunohistochemical and FCM analyses revealed that the development and distribution of thymic ECs and TECs were unchanged in *Cldn5*$^{-/-}$ mice (Fig. 4A and Supplementary Figure S5). The total thymocyte number, live cell percentage and overall thymocyte development determined by CD4 and CD8α FCM staining were comparable between control and *Cldn5*$^{-/-}$ mice (Fig. 4B and Supplementary Figure S5). No obvious morphological abnormalities were observed in the TJ structures of *Cld5*$^{-/-}$ thymic EC according to electron microscopy images (Fig. 4C). These observations are consistent with the phenotypes of *Cld5*$^{-/-}$ brain (39) and might be explained by other TJ molecules such as JAM-A that maintain membrane appositions (49). We then examined the permeability of the thymic vasculatures using a primary amine-reactive biotinylation reagent (M.W.

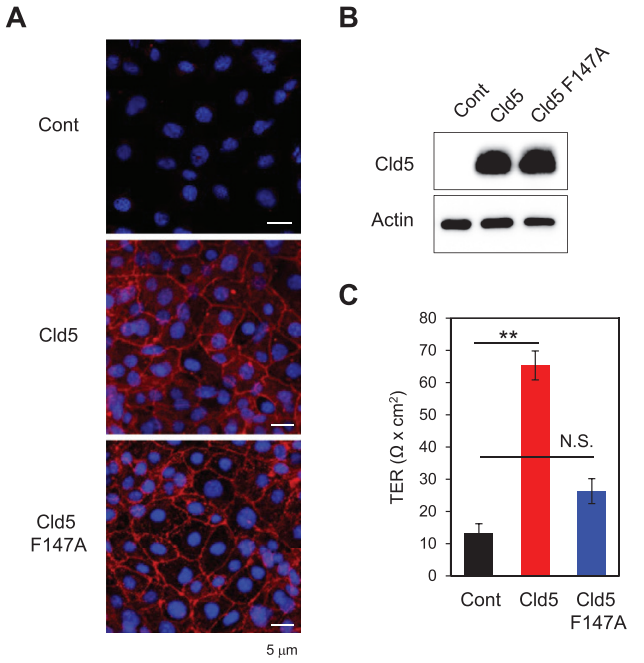

Fig. 3. Tight junction-forming capability of Cld5 is required for controlling paracellular permeability of cultured endothelial cells. SVECs were retrovirally transfected with control vector (Cont), *Cldn5*-ligated vector (Cld5) or *Clnd5* F147A mutant-ligated vector (Cld5 F147A). Stable clones were established and examined by immunofluorescence (A) and western blotting (B) analyses with anti-Cld5 antibody. (C) TER of confluent SVECs stably expressing one of the above vectors was measured 5 days after cell seeding in trans-wells. Student's *t*-test was performed between Cont and Cld5, and Cont and Cld5F147A. $^{**}P < 0.01$; N.S., not significant.

607), which covalently cross-links to accessible proteins and is commonly used to evaluate the permeability of TJs of epithelial cells and ECs *in vivo* (39, 50). In contrast to WT mice, the tracer was diffusely distributed in the parenchyma of the cortex in *Cld5*$^{-/-}$ mice, indicating that the endothelial barrier in the thymus of *Cld5*$^{-/-}$ mice was impaired (Fig. 4D). These results indicate that Cld5 plays a crucial role in the establishment of the BTB in the cortex.

Blood-borne molecules enter from Cld5^{-} *vessels into the thymic medulla*

The specific absence of Cld5 in the thymic vessels at the medulla and CMJ might be associated with the distinct permeability of blood-borne molecules in the cortex and medulla, as reported previously (9, 27). We therefore performed an *in vivo* tracer assay using adult mice, in which the medullary regions are well developed. Thirty minutes after the i.v. injection, the biotin tracer was excluded from the cortical parenchyma but retained within the blood vessels (Fig. 5A), consistent with E18 embryos (Fig. 4A). In contrast, the biotin tracer was leaked into the medulla and CMJ (Fig. 5A), consistent with previous reports (9, 27). The thymic vascular network possesses a conduit system that is composed of ECM for the transport of blood-borne molecules to tissue parenchyma (31). Both Cld5^{+} and Cld5^{-} large vessels at the CMJ were surrounded by double-walled ECM that included laminin and collagen IV and formed perivascular spaces (14, 31) (Supplementary Figure S6). While Cld5^{+} large vessels retained tracer molecules inside of the lumen, the biotin tracer penetrated through Cld5^{-} large vessels at the CMJ, and leaked tracers were co-localized with the laminin staining (Fig. 5A). Next, we used S1P (M.W. 380), which exists abundantly in the bloodstream and is a key lipid mediator for the egress of mature SP thymocytes from the medulla (17, 21, 24), as a physiological tracer. Tetramethylrhodamine-conjugated S1P (M.W. 807) was distributed diffusely in the medullary region, but not in the cortical area (Fig. 5B). It was noted that blood-borne S1P did not enter the conduit system but was detected intensively around Cld5^{-} vessels at the CMJ, whereas no such signals were observed in Cld5^{+} large vessels or cortical capillaries (Fig. 5B). These results indicate that the BTB is established in the cortical region, where Cld5^{+} capillaries exist. In addition, blood-borne molecules enter the medullary regions from Cld5^{-} vessels at the medulla and CMJ via simple diffusion or the conduit system, probably depending on the properties of the molecules (Supplementary Figure S7).

Thymocytes egress from Cld5^{-} *vessels into blood circulation*

Mature thymocytes egress from blood vessels at the CMJ according to the S1P gradient (24). We therefore examined whether mature thymocytes migrate from Cld5^{-} vessels to the periphery. We found that CD3ε^{high} mature thymocytes attached specifically in the lumen of Cld5^{-} large vessels but rarely in the lumen of Cld5^{+} vessels at the CMJ (Fig. 6A). Quantification analysis indicated that all attached CD3ε^{high} mature thymocytes were detected with Cld5^{-} large vessels (19/19, or 100%), but not at all with Cld5^{+} vessels (0/19, or 0%). In addition, intravascular labeling analysis (43) demonstrated that egressing mature thymocytes, which were labeled shortly after the i.v. injection of anti-CD4 antibodies, were detected specifically in the lumen of Cld5^{-} vessels (Fig. 6B). Furthermore, when mice were treated with FTY720, an inhibitor of thymocyte egress (44, 48), we observed an accumulation of CD3ε^{high} mature thymocytes in the perivascular spaces of Cld5^{-} vessels, but not in those of Cld5^{+} vessels (Fig. 6C). These results indicated that mature thymocytes were exported to the blood circulation selectively from the Cld5^{-} vessels, thus generating a plasma-derived S1P gradient (Supplementary Figure S7).

Discussion

The current study found that Cld5, a crucial component of the BBB in the central nervous system (35), is heterogeneously expressed in thymic ECs: nearly all ECs in the cortical capillaries and αSMA^{+} arterioles expressed Cld5, whereas nearly half of ECs in the vessels of the medulla/CMJ specifically lacked Cld5 expression. We further observed that i.v.-injected tracers were retained within cortical Cld5^{+} vessels but entered the thymic medulla from Cld5^{-} vessels. Cld5 overexpression in ECs decreased paracellular permeability *in vitro*. Furthermore, blood-borne molecules were leaked into the cortical parenchyma of *Cldn5*$^{-/-}$ thymus *in vivo*. These results strongly suggest that Cld5 is directly involved

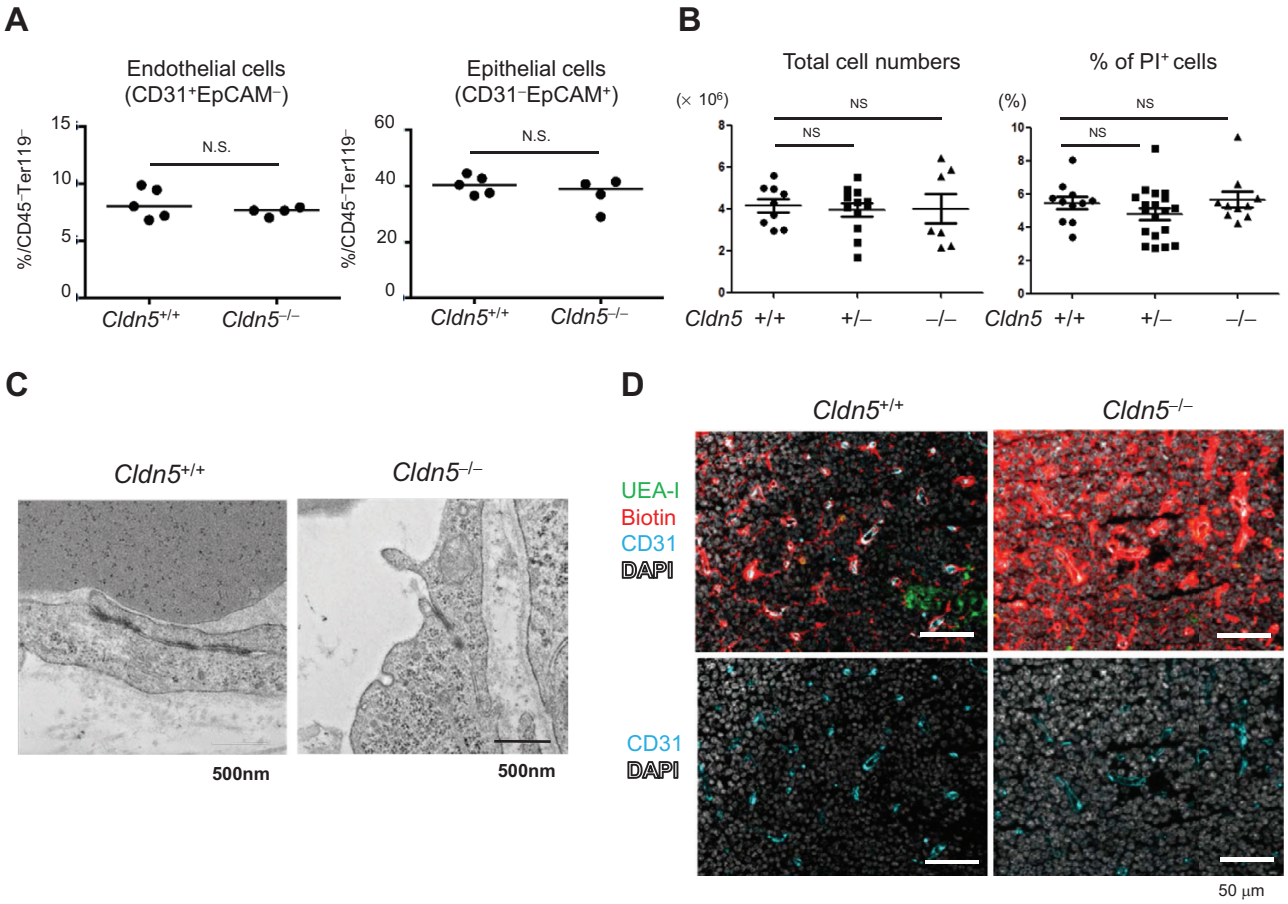

Fig. 4. Cld5 is a crucial component of the blood–thymus barrier. Thymi from *Cldn5*$^{+/+}$, *Cldn5*$^{+/-}$ and *Cldn5*$^{-/-}$ mice were analyzed at E18.5. (A) Enzymatically digested total thymic cells from *Cldn5*$^{+/+}$ and *Cldn5*$^{-/-}$ mice were stained with anti-CD45, Ter119, CD31 and EpCAM antibodies and analyzed by FCM. The percentages of endothelial and epithelial cells in the CD45^{-}Ter119^{-} fraction are indicated. Horizontal bars indicate median values. Statistical significance was analyzed by using the Mann–Whitney test; N.S., not significant. (B) Total thymocyte numbers and percentages of PI^{+} dead cells in total thymocytes were analyzed. (C) TJ morphologies in the cortical capillaries were examined by using electron microscopy. (D) The distribution of an i.v.-injected biotin tracer was detected by Avidin staining. The data are representative of at least five independent experiments.

in regulating the permeability of the thymic vasculature and plays a crucial role in establishing the BTB. In addition, the absence of Cld5 in specific vessels, probably PCVs, located at the medulla/CMJ, may ensure the specific gateway for blood-borne molecules to enter the medullary regions.

Our results showed that Cld5^{-} vessels at the medulla/CMJ are the entry site for blood-borne molecules, and that this entry could affect negative selection and T_{reg} cell induction (27). Interestingly, an i.v.-injected biotin tracer labeled the ECM forming double-walled perivascular spaces (11, 14), indicating that at least some blood-borne proteins entering the thymic medullary parenchyma via a conduit system (31) originate from Cld5^{-} vessels, although the functional importance of the thymic conduit system itself remains to be proved. On the other hand, the BTB, which blocks the entry of blood-borne molecules into the cortex, is suggested to play a role in eliminating the effect of extrathymic antigens on positive selection (9). Although claudins play crucial roles not only in regulating paracellular permeability, but also in controlling cell conditions including cell signaling, proliferation and migration (51, 52), our *in vitro* data using Cld5 mutant (F147A) confirmed that Cld5 directly controls the barrier function of TJs in ECs. We found no visible short-term effects on thymocyte selection in *Cldn5*$^{-/-}$ embryos. Because these pups died soon after birth, we could not evaluate any long-term effects of a defective BTB on T-cell development and/or maintenance of thymic microenvironments with age.

S1P, a crucial lipid mediator for the egress of newly developed T cells in the thymus (17, 21, 24, 53), also enters the thymus from Cld5^{-} vessels to create a blood-derived S1P gradient. Consistently, we found here that CD3ε^{high} mature thymocytes attached specifically in the lumen of Cld5^{-} vessels in the thymus. A previous study found that the overexpression of S1P1 in immature thymocytes is sufficient for the export of immature thymocytes from the cortex on the basis of the S1P gradient generated from PDGFRβ^{+} pericytes surrounding the cortical capillaries (20, 43). However, the same study also noted a strikingly unusual perivascular accumulation of thymocytes in the cortical capillaries. Considering that Cld5^{+} vessels are dominant in the cortex, the enlargement of perivascular spaces in the cortex may suggest that cortical Cld5^{+} vessels are an inefficient gateway for S1P to enter from the

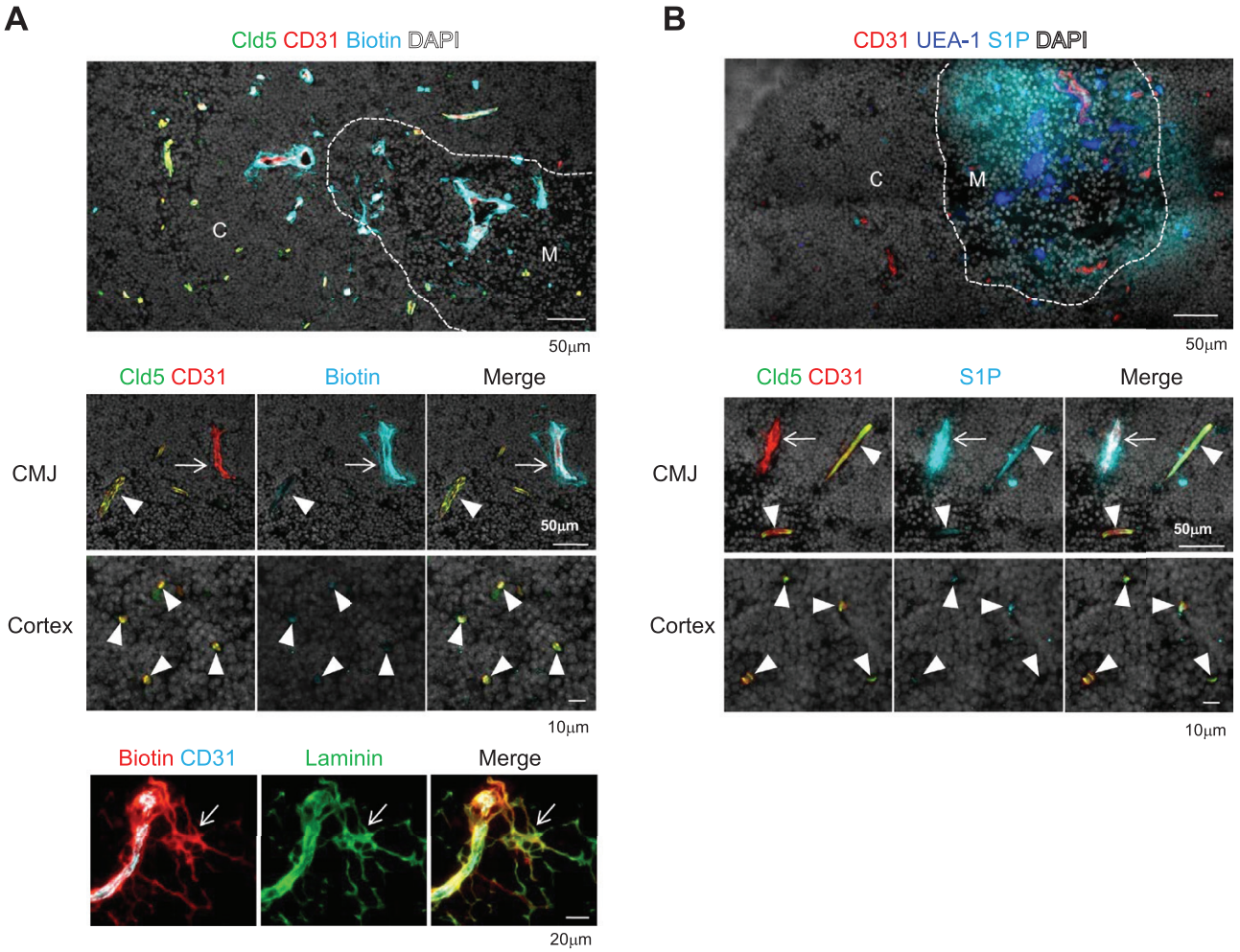

Fig. 5. Leakage of blood-borne molecules from Cld5⁻ vessels in the medulla and CMJ. 6- to 8-week-old B6 mice were i.v.-injected with biotin-compound tracer (A) or tetramethylrhodamine-conjugated S1P (B) as described in the "Methods" section. (A) The thymus was removed 30 min after the biotin injection and immunostained by anti-Cld5 antibody, anti-CD31 antibody and streptavidin (upper and middle panels) or anti-CD31, laminin and streptavidin (lower panel). (B) The thymus was removed 5 min (upper panel) and 30 min (lower panels) after S1P injection and examined by immunohistochemistry using anti-CD31 antibody and a medulla marker, UEA1. Dotted lines indicate borders between the cortex (C) and medulla (M) defined by DAPI staining. Arrowheads and arrows indicate Cld5⁺ and Cld5⁻ vessels, respectively. These data are representative of at least three independent experiments.

blood circulation. S1P transporters such as Spns2 expressed in ECs and S1P-degrading enzymes such as LPP3 also play a role in generating the S1P gradient as well as thymocyte egress (54, 55). In addition to the leakage of blood S1P from Cld5⁻ vessels, these other mechanisms might be independently operated and required for the generation of the optimal S1P gradient in the thymus to regulate thymocyte egress. It remains to be seen whether a deficiency in Cld5 has a mechanistic role in cellular traffic. In any case, the Cld5-based BTB in the cortex and the specific gateway to the blood circulation via Cld5⁻ vessels at the medulla/CMJ may be the basis of a mechanism that ensures the efficient export of mature SP thymocytes from the medulla to the periphery.

The recruitment of various cellular components into the thymus is also important for T-cell development. Lymphoid progenitors enter the postnatal thymus through the blood vessels at the CMJ (3). We found Cld5 expression in blood vessels with large diameters at the CMJ was heterogeneous, and CD62P, which contributes to the recruitment of adult thymic progenitors (14, 56), was weakly expressed in both Cld5⁻ and Cld5⁺ vessels, but not in cortical ECs (data not shown). Self-antigen-incorporated DCs also migrate into the thymic medulla from the periphery and play a role in central tolerance induction, although their entry sites were not addressed (26, 57, 58). Thus, whether Cld5⁻ vessels are the entry site for various cellular components into the thymus, and, if so, how Cld5 expression regulates the process remain to be investigated.

In ontogeny, Cld5⁻ ECs are first observed around E17-18, when mature CD4 SP thymocytes develop and the medullary regions expand, suggesting a close association between the development of Cld5⁻ vessels and mTEC maturation. This notion is consistent with an analysis of the anatomy of the thymic vasculature, which found a close physical association of PCVs and mTECs (10). High endothelial venules, which are the entry site for naive T cells

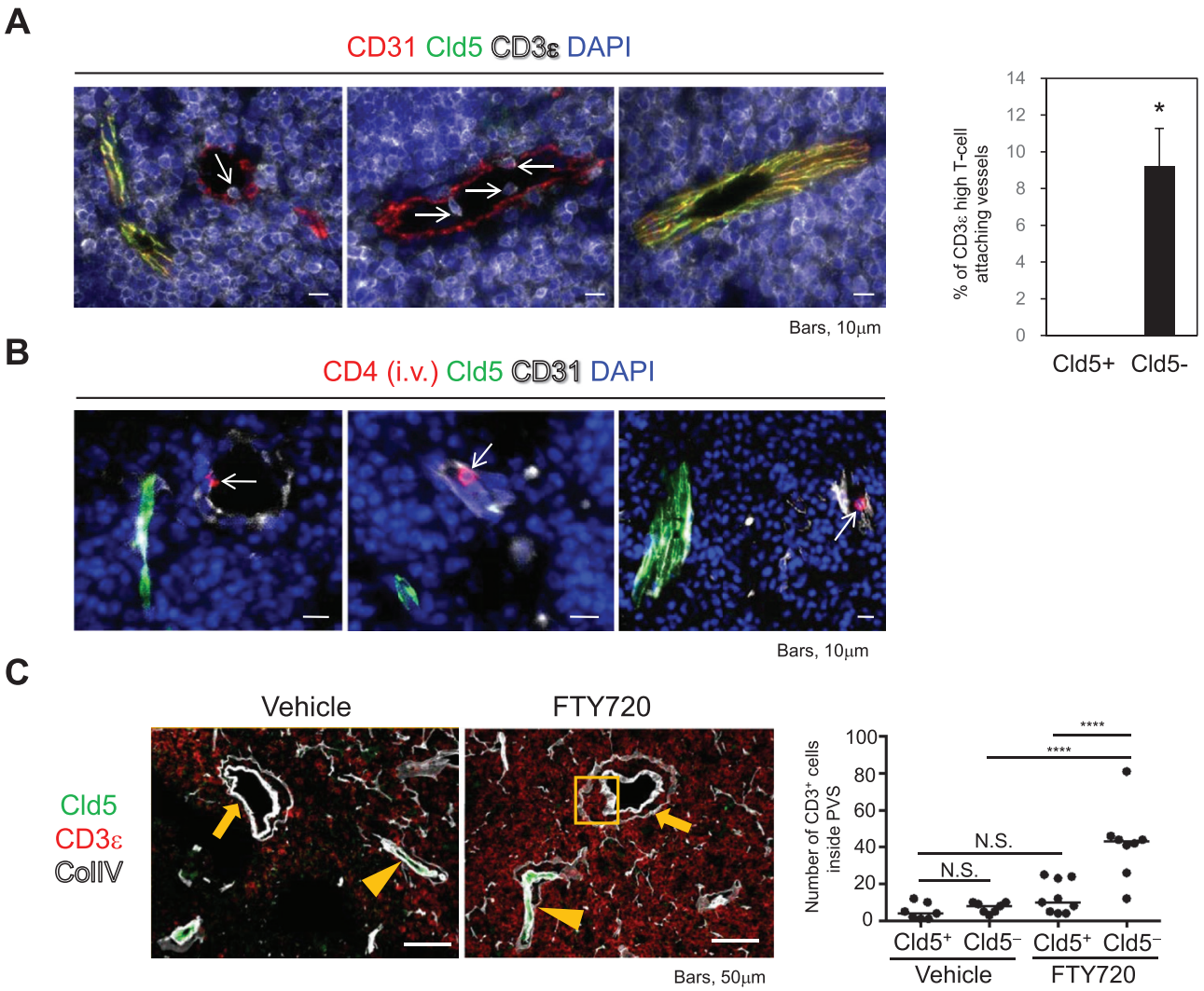

Fig. 6. CD3ε^{high} mature thymocytes egress from Cld5$^-$ blood vessels. (A) Thymic tissues were immune-stained with anti-CD31, Cld5 and CD3ε antibodies. Arrows indicate CD3ε^{high} lymphocytes attaching to the lumen of Cld5$^-$ blood vessels around the CMJ (left). The means and SEM of the percentage of CD3ε^{high} T-cell-attaching Cld5$^+$ or Cld5$^-$ blood vessels in the medulla/CMJ (right). *$P < 0.05$, as determined by two-tailed Student's *t*-test. (B) Adult C57BL/6 mice were i.v.-injected with PE-conjugated anti-CD4 mAb, and thymi were removed 3 min after the injection. CD4-labeled egressing thymocytes were identified in the lumen of Cld5$^-$ vessels in the medulla and CMJ. Arrows indicate egressing thymocytes. These data are representative of at least five independent experiments. (C) Adult C57BL/6 mice were treated with FTY720 for 25 consecutive days, and thymi were examined for immunohistochemistry. Arrowheads and arrows indicate Cld5$^+$ and Cld5$^-$ vessels, respectively. The squared area shows the accumulation of egressing thymocytes in the perivascular space (PVS) of Cld5$^-$ blood vessels. Representative data are shown ($n = 2$ per group). The number of CD3$^+$ cells inside the PVS was counted and compared between Cld5$^+$ and Cld5$^-$ vessels with or without FTY720 treatment. Lines indicate medians. Statistical significance was evaluated by one-way ANOVA. ****$P < 0.0001$, N.S., not significant.

into lymph nodes, also lack Cld5 expression (47), and their formation is controlled by LTβR and the downstream non-canonical nuclear factor kB pathway activated by DCs (59–61). In the thymus, these signals are provided by SP cells, LTi cells and γδ T cells to promote mTEC differentiation and maturation (1). Thus, the possibility that these signals could also trigger the generation of Cld5$^-$ thymic vessels in ontogeny is intriguing. The proportion of Cld5$^+$ ECs significantly decreases with age, possibly because of a reduction of the cortical compartment during thymic involution (62). The expression levels of Cld5 in thymic ECs also decrease with age. Foxn1$^{Δ/Δ}$ thymi show leaky vessels (63). Therefore, the age-related decrease in Foxn1 expression in TECs (64–66) may explain the decreased Cld5 expression in thymic ECs. Furthermore, the age-related increase in TGFβ (67) which also decreases Cld5 expression in ECs (68), could also be involved in the gradual decrease in Cld5 expression in thymic ECs. In either case, whether the decrease in Cld5 expression in ECs with age affects the homeostasis of the thymic microenvironment remains to be investigated.

In summary, we provide molecular evidence that Cld5-mediated TJs ensure the BTB in the cortex compartment. An absence of Cld5 expression in the medulla and CMJ may allow the entrance of blood-borne molecules including S1P into the thymic medulla to ensure the trafficking of mature

thymocytes into blood circulation as well as antigens for central tolerance induction.

Funding

This work was supported by JSPS KAKENHI [grant numbers JP15H01154, JP18H02640, 18K19442 to Y.H.; JP19K07617 and JP12J03485 (research fellowship) to T.N.; JP20H00534 and JP15H05790 to J.K.; JP19K07513 to M.I.; JP18H06232, JP19K21331 and JP20K16281 to T.I. and 20K06469 to K.K.], the Takeda Science Foundation to Y.H., AMED under grant number JP20gm5010001 to Y.H. and iPS Cell Research Fund to Y.H.

Acknowledgements

We thank Dr M. Miyasaka (Laboratory of Immunodynamics, World Premier International Immunology Frontier Research Center, Osaka University) for providing the SVEC line, Mr Koda and Mrs Furuta for the electron microscopic analysis, and Dr P. Karagiannis for proof reading. *Cldn5*$^{-/-}$ mice were provided by the late Prof. Shoichiro Tsukita. We also thank members of our laboratory for technical advice and helpful discussion.

Conflicts of interest statement: the authors declared no conflicts of interest.

References

1 Abramson, J. and Anderson, G. 2017. Thymic epithelial cells. *Annu. Rev. Immunol.* 35:85.
2 Hamazaki, Y., Sekai, M. and Minato, N. 2016. Medullary thymic epithelial stem cells: role in thymic epithelial cell maintenance and thymic involution. *Immunol. Rev.* 271:38.
3 Takahama, Y. 2006. Journey through the thymus: stromal guides for T-cell development and selection. *Nat. Rev. Immunol.* 6:127.
4 Anderson, G. and Takahama, Y. 2012. Thymic epithelial cells: working class heroes for T cell development and repertoire selection. *Trends Immunol.* 33:256.
5 Klein, L., Hinterberger, M., Wirnsberger, G. and Kyewski, B. 2009. Antigen presentation in the thymus for positive selection and central tolerance induction. *Nat. Rev. Immunol.* 9:833.
6 Love, P. E. and Bhandoola, A. 2011. Signal integration and crosstalk during thymocyte migration and emigration. *Nat. Rev. Immunol.* 11:469.
7 Petrie, H. T. 2002. Role of thymic organ structure and stromal composition in steady-state postnatal T-cell production. *Immunol. Rev.* 189:8.
8 Weinreich, M. A. and Hogquist, K. A. 2008. Thymic emigration: when and how T cells leave home. *J. Immunol.* 181:2265.
9 Raviola, E. and Karnovsky, M. J. 1972. Evidence for a blood-thymus barrier using electron-opaque tracers. *J. Exp. Med.* 136:466.
10 Anderson, M., Anderson, S. K. and Farr, A. G. 2000. Thymic vasculature: organizer of the medullary epithelial compartment? *Int. Immunol.* 12:1105.
11 Kato, S. 1997. Thymic microvascular system. *Microsc. Res. Tech.* 38:287.
12 Kato, S. and Schoefl, G. I. 1989. Microvasculature of normal and involuted mouse thymus. Light- and electron-microscopic study. *Acta Anat. (Basel)* 135:1.
13 Lind, E. F., Prockop, S. E., Porritt, H. E. and Petrie, H. T. 2001. Mapping precursor movement through the postnatal thymus reveals specific microenvironments supporting defined stages of early lymphoid development. *J. Exp. Med.* 194:127.
14 Mori, K., Itoi, M., Tsukamoto, N., Kubo, H. and Amagai, T. 2007. The perivascular space as a path of hematopoietic progenitor cells and mature T cells between the blood circulation and the thymic parenchyma. *Int. Immunol.* 19:745.
15 Törö, I. and Oláh, I. 1967. Penetration of thymocytes into the blood circulation. *J. Ultrastruct. Res.* 17:439.
16 Ushiki, T. 1986. A scanning electron-microscopic study of the rat thymus with special reference to cell types and migration of lymphocytes into the general circulation. *Cell Tissue Res.* 244:285.
17 Pappu, R., Schwab, S. R., Cornelissen, I. *et al.* 2007. Promotion of lymphocyte egress into blood and lymph by distinct sources of sphingosine-1-phosphate. *Science* 316:295.
18 Ernström, U., Glyllensten, L. and Larsson, B. 1965. Venous output of lymphocytes from the thymus. *Nature* 207:540.
19 Kotani, M., Seiki, K., Yamashita, A. and Horii, I. 1966. Lymphatic drainage of thymocytes to the circulation in the guinea pig. *Blood* 27:511.
20 Cyster, J. G. and Schwab, S. R. 2012. Sphingosine-1-phosphate and lymphocyte egress from lymphoid organs. *Annu. Rev. Immunol.* 30:69.
21 Matloubian, M., Lo, C. G., Cinamon, G. *et al.* 2004. Lymphocyte egress from thymus and peripheral lymphoid organs is dependent on S1P receptor 1. *Nature* 427:355.
22 Allende, M. L., Dreier, J. L., Mandala, S. and Proia, R. L. 2004. Expression of the sphingosine 1-phosphate receptor, S1P1, on T-cells controls thymic emigration. *J. Biol. Chem.* 279:15396.
23 Carlson, C. M., Endrizzi, B. T., Wu, J. *et al.* 2006. Kruppel-like factor 2 regulates thymocyte and T-cell migration. *Nature* 442:299.
24 Yanagida, K. and Hla, T. 2017. Vascular and immunobiology of the circulatory sphingosine 1-phosphate gradient. *Annu. Rev. Physiol.* 79:67.
25 Marshall, A. H. and White, R. G. 1961. The immunological reactivity of the thymus. *Br. J. Exp. Pathol.* 42:379.
26 Kyewski, B. A., Fathman, C. G. and Kaplan, H. S. 1984. Intrathymic presentation of circulating non-major histocompatibility complex antigens. *Nature* 308:196.
27 Atibalentja, D. F., Byersdorfer, C. A. and Unanue, E. R. 2009. Thymus-blood protein interactions are highly effective in negative selection and regulatory T cell induction. *J. Immunol.* 183:7909.
28 Hadeiba, H., Lahl, K., Edalati, A. *et al.* 2012. Plasmacytoid dendritic cells transport peripheral antigens to the thymus to promote central tolerance. *Immunity* 36:438.
29 Liblau, R. S., Tisch, R., Shokat, K. *et al.* 1996. Intravenous injection of soluble antigen induces thymic and peripheral T-cells apoptosis. *Proc. Natl Acad. Sci. USA* 93:3031.
30 Murphy, K. M., Heimberger, A. B. and Loh, D. Y. 1990. Induction by antigen of intrathymic apoptosis of $CD4^+CD8^+TCRlo$ thymocytes *in vivo*. *Science* 250:1720.
31 Drumea-Mirancea, M., Wessels, J. T., Müller, C. A. *et al.* 2006. Characterization of a conduit system containing laminin-5 in the human thymus: a potential transport system for small molecules. *J. Cell Sci.* 119(Pt 7):1396.
32 Rahimi, N. 2017. Defenders and challengers of endothelial barrier function. *Front. Immunol.* 8:1847.
33 Dejana, E. 2004. Endothelial cell-cell junctions: happy together. *Nat. Rev. Mol. Cell Biol.* 5:261.
34 Tsukita, S., Furuse, M. and Itoh, M. 2001. Multifunctional strands in tight junctions. *Nat. Rev. Mol. Cell Biol.* 2:285.
35 Morita, K., Sasaki, H., Furuse, M. and Tsukita, S. 1999. Endothelial claudin: claudin-5/TMVCF constitutes tight junction strands in endothelial cells. *J. Cell Biol.* 147:185.
36 Castro Dias, M., Coisne, C., Baden, P. *et al.*; German Mouse Clinic Consortium. 2019. Claudin-12 is not required for blood-brain barrier tight junction function. *Fluids Barriers CNS* 16:30.
37 Rubin, L. L. and Staddon, J. M. 1999. The cell biology of the blood-brain barrier. *Annu. Rev. Neurosci.* 22:11.
38 Pardridge, W. M. 1998. *Introduction to the Blood-Brain Barrier. Methodology, Biology and Pathology*, p. 1. Cambridge University Press, Cambridge, UK.
39 Nitta, T., Hata, M., Gotoh, S. *et al.* 2003. Size-selective loosening of the blood-brain barrier in claudin-5-deficient mice. *J. Cell Biol.* 161:653.
40 Hamazaki, Y., Fujita, H., Kobayashi, T. *et al.* 2007. Medullary thymic epithelial cells expressing Aire represent a unique lineage derived from cells expressing claudin. *Nat. Immunol.* 8:304.

41 Seach, N., Wong, K., Hammett, M., Boyd, R. L. and Chidgey, A. P. 2012. Purified enzymes improve isolation and characterization of the adult thymic epithelium. *J. Immunol. Methods* 385:23.
42 Sekai, M., Hamazaki, Y. and Minato, N. 2014. Medullary thymic epithelial stem cells maintain a functional thymus to ensure lifelong central T cell tolerance. *Immunity* 41:753.
43 Zachariah, M. A. and Cyster, J. G. 2010. Neural crest-derived pericytes promote egress of mature thymocytes at the corticomedullary junction. *Science* 328:1129.
44 Yagi, H., Kamba, R., Chiba, K. *et al.* 2000. Immunosuppressant FTY720 inhibits thymocyte emigration. *Eur. J. Immunol.* 30:1435.
45 O'Connell, K. A. and Edidin, M. 1990. A mouse lymphoid endothelial cell line immortalized by simian virus 40 binds lymphocytes and retains functional characteristics of normal endothelial cells. *J. Immunol.* 144:521.
46 Lampugnani, M. G., Corada, M., Caveda, L. *et al.* 1995. The molecular organization of endothelial cell to cell junctions: differential association of plakoglobin, beta-catenin, and alpha-catenin with vascular endothelial cadherin (VE-cadherin). *J. Cell Biol.* 129:203.
47 Pfeiffer, F., Kumar, V., Butz, S. *et al.* 2008. Distinct molecular composition of blood and lymphatic vascular endothelial cell junctions establishes specific functional barriers within the peripheral lymph node. *Eur. J. Immunol.* 38:2142.
48 Piontek, J., Winkler, L., Wolburg, H. *et al.* 2008. Formation of tight junction: determinants of homophilic interaction between classic claudins. *FASEB J.* 22:146.
49 Otani, T., Nguyen, T. P., Tokuda, S. *et al.* 2019. Claudins and JAM-A coordinately regulate tight junction formation and epithelial polarity. *J. Cell Biol.* 218:3372.
50 Furuse, M., Hata, M., Furuse, K. *et al.* 2002. Claudin-based tight junctions are crucial for the mammalian epidermal barrier: a lesson from claudin-1-deficient mice. *J. Cell Biol.* 156:1099.
51 Kawai, Y., Hamazaki, Y., Fujita, H. *et al.* 2011. Claudin-4 induction by E-protein activity in later stages of CD4/8 double-positive thymocytes to increase positive selection efficiency. *Proc. Natl Acad. Sci. USA* 108:4075.
52 Tiwari-Woodruff, S. K., Buznikov, A. G., Vu, T. Q. *et al.* 2001. OSP/claudin-11 forms a complex with a novel member of the tetraspanin super family and beta1 integrin and regulates proliferation and migration of oligodendrocytes. *J. Cell Biol.* 153:295.
53 Schwab, S. R., Pereira, J. P., Matloubian, M., Xu, Y., Huang, Y. and Cyster, J. G. 2005. Lymphocyte sequestration through S1P lyase inhibition and disruption of S1P gradients. *Science* 309:1735.
54 Fukuhara, S., Simmons, S., Kawamura, S. *et al.* 2012. The sphingosine-1-phosphate transporter Spns2 expressed on endothelial cells regulates lymphocyte trafficking in mice. *J. Clin. Invest.* 122:1416.
55 Bréart, B., Ramos-Perez, W. D., Mendoza, A. *et al.* 2011. Lipid phosphate phosphatase 3 enables efficient thymic egress. *J. Exp. Med.* 208:1267.
56 Rossi, F. M., Corbel, S. Y., Merzaban, J. S. *et al.* 2005. Recruitment of adult thymic progenitors is regulated by P-selectin and its ligand PSGL-1. *Nat. Immunol.* 6:626.
57 Baba, T., Nakamoto, Y. and Mukaida, N. 2009. Crucial contribution of thymic Sirp alpha$^+$ conventional dendritic cells to central tolerance against blood-borne antigens in a CCR2-dependent manner. *J. Immunol.* 183:3053.
58 Proietto, A. I., van Dommelen, S., Zhou, P. *et al.* 2008. Dendritic cells in the thymus contribute to T-regulatory cell induction. *Proc. Natl Acad. Sci. USA* 105:19869.
59 Drayton, D. L., Bonizzi, G., Ying, X., Liao, S., Karin, M. and Ruddle, N. H. 2004. I kappa B kinase complex alpha kinase activity controls chemokine and high endothelial venule gene expression in lymph nodes and nasal-associated lymphoid tissue. *J. Immunol.* 173:6161.
60 Onder, L., Danuser, R., Scandella, E. *et al.* 2013. Endothelial cell-specific lymphotoxin-beta receptor signaling is critical for lymph node and high endothelial venule formation. *J. Exp. Med.* 210:465.
61 Moussion, C. and Girard, J. P. 2011. Dendritic cells control lymphocyte entry to lymph nodes through high endothelial venules. *Nature* 479:542.
62 Lynch, H. E., Goldberg, G. L., Chidgey, A., Van den Brink, M. R., Boyd, R. and Sempowski, G. D. 2009. Thymic involution and immune reconstitution. *Trends Immunol.* 30:366.
63 Bryson, J. L., Griffith, A. V., Hughes, B. 3rd *et al.* 2013. Cell-autonomous defects in thymic epithelial cells disrupt endothelial-perivascular cell interactions in the mouse thymus. *PLoS ONE* 8:e65196.
64 Ortman, C. L., Dittmar, K. A., Witte, P. L. and Le, P. T. 2002. Molecular characterization of the mouse involuted thymus: aberrations in expression of transcription regulators in thymocyte and epithelial compartments. *Int. Immunol.* 14:813.
65 Zook, E. C., Krishack, P. A., Zhang, S. *et al.* 2011. Overexpression of Foxn1 attenuates age-associated thymic involution and prevents the expansion of peripheral CD4 memory T cells. *Blood* 118:5723.
66 Chen, L., Xiao, S. and Manley, N. R. 2009. Foxn1 is required to maintain the postnatal thymic microenvironment in a dosage-sensitive manner. *Blood* 113:567.
67 Hauri-Hohl, M. M., Zuklys, S., Keller, M. P. *et al.* 2008. TGF-beta signaling in thymic epithelial cells regulates thymic involution and postirradiation reconstitution. *Blood* 112:626.
68 Watabe, T., Nishihara, A., Mishima, K. *et al.* 2003. TGF-beta receptor kinase inhibitor enhances growth and integrity of embryonic stem cell-derived endothelial cells. *J. Cell Biol.* 163:1303.